Field emission of electrons from a Cs-doped single carbon nanotube of known chiral indices

Gongpu Zhao, Qi Zhang, Han Zhang, Guang Yang, Otto Zhou, and Lu-Chang Qin[a)]
Department of Physics and Astronomy, University of North Carolina at Chapel Hill, Chapel Hill, North Carolina 27599-3255 and Curriculum in Applied and Materials Sciences, University of North Carolina at Chapel Hill, Chapel Hill, North Carolina 27599-3255

Jie Tang
National Institute for Materials Science, Tsukuba 305-0047, Japan

(Received 8 October 2006; accepted 20 November 2006; published online 29 December 2006)

The authors report the effects of Cs doping on the field emission properties of a five-shell single carbon nanotube. The chiral indices of each shell of this carbon nanotube have been determined using nanobeam electron diffraction, which has four semiconducting shells and one metallic shell in the middle. From the Fowler-Nordheim plots, a reduction from 4.8 to 3.8 eV has been observed in the work function of the single carbon nanotube before and after Cs doping. © *2006 American Institute of Physics*. [DOI: 10.1063/1.2420796]

Carbon nanotubes have attracted considerable interest as future field emission electron sources due to their high aspect ratio and robust structure.[1–3] Carbon nanotubes can be used in a wide range of applications requiring electron emission such as flat panel displays, point electron sources, and x-ray sources.[4–6] It has been shown that carbon nanotubes have excellent field emission properties such as high brightness,[5] low turn on field,[3] narrow energy distribution,[7] and good stability.[8] However, one disadvantage in using carbon nanotubes is that its work function is high (4.6–5 eV),[9,10] which makes it difficult for electrons to escape and effectively limit the temporal coherence imposed by the energy spread that is ultimately linked to the work function of the emitter.[11] Cesium (Cs) deposition has been widely used in vacuum microelectronic devices.[12–14] For large area field emission arrays, Cs vapor coating is a good way to deposit Cs atoms onto the emitters. It has been reported that Cs intercalation in carbon nanotube bundles reduced their work function from 4.8 to 2.4 eV and that the structure is stable in ultrahigh vacuum during electron emission.[15–17] In this letter, we report the effect of Cs doping on the field emission properties of a single multiwalled carbon nanotube of known chiral indices.

The individual carbon nanotube was grown inside a micron-size carbon fiber by a chemical vapor deposition method.[18] A single carbon fiber was picked up and attached to a tungsten supporting tip and then this fiber was fractured by a mechanical force to expose the contained carbon nanotube. Figure 1(a) is a transmission electron microscope (TEM) image which shows a single carbon nanotube of length 0.6 μm and diameter 8 nm extruded from the carbon fiber.

We used nanobeam electron diffraction to determine the chiral indices (u,v) of each shell of the carbon nanotube.[19–24] The perimeter vector of each individual shell is defined by $\mathbf{A}=(u,v)=u\mathbf{a}_1+v\mathbf{a}_2$, where $\mathbf{a}_1$ and $\mathbf{a}_2$ ($a_1=a_2=0.246$ nm) are the basis vectors of graphene with an interangle of 60°. Once they are known, the metallicity of the shell can be told from its chiral indices (u,v): if $(u-v)/3$ is integer, it is metallic and otherwise it is semiconducting. The nanobeam electron diffraction experiments were carried out in a JEM-2010F TEM operated at 80 kV. The diffraction pattern [Fig. 1(b)] was recorded on a charge-coupled device camera with the camera length of 30 cm and exposure time of 30 s. From the TEM images, the inner and outer diameters of this carbon nanotube were estimated to be about 4 and 8 nm, respectively. The chiral indices (u,v) were determined from the ratios of $v/u=(2D_2-D_1)/(2D_1-D_2)$ for each shell, where D_1 and D_2 are the layer line spacings measured in the electron diffraction pattern.[22,23] By this method, all the possible

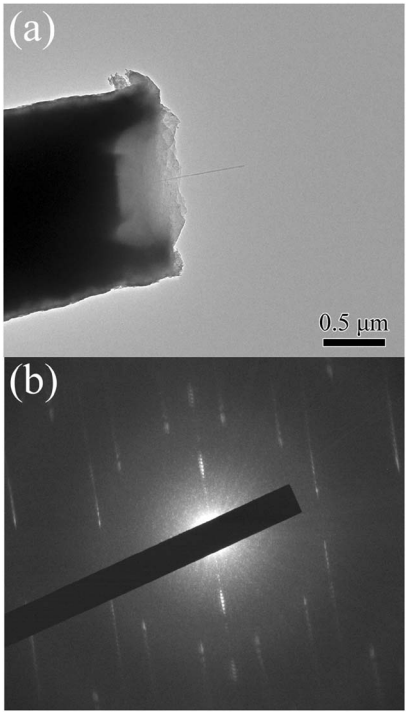

FIG. 1. (a) TEM image of a single carbon nanotube extruding from a carbon fiber of 1.3 μm diameter. The inner diameter and the outer diameter of this carbon nanotube were about 4 and 8 nm, respectively. (b) Nanobeam electron diffraction pattern of the carbon nanotube. The diffraction pattern suggests that all the shells have nearly the same helicity.

[a)]Electronic mail: lcqin@physics.unc.edu

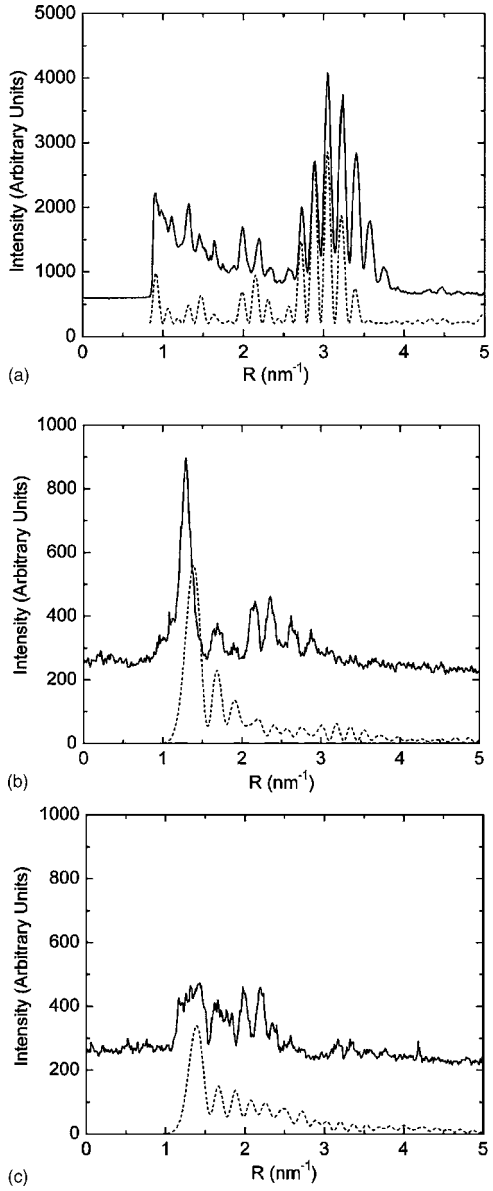

FIG. 2. (a) Experimental (solid line) and calculated (dash line) intensity profiles on the equatorial layer line. (b) Experimental (solid line) and calculated (dash line) intensity profiles $I(R,\Phi+\pi,l_1)$. (c) Experimental (solid line) and simulated (dash line) intensity profiles $I(R,\Phi,l_1)$. Asymmetry of the two patterns is observed due to interferences of the two layer lines from the second and the fourth shell that have the same helicity.

v/u ratios were measured to be 0.3793, 0.3810, 0.3846, 0.3889, 0.3913, 0.3929, 0.4000, and 0.4091. The exact shell number j and the diameter d_j of each shell were determined with the assistance of simulating the intensities on the equatorial layer line. The scattering amplitude on the equatorial layer line from a single shell can be expressed by $F(R)=fdJ_0(\pi dR)$, where d is the diameter of the shell and f is the atomic scattering factor of carbon for electrons. For a multiwalled carbon nanotube, the scattered amplitude for equatorial line is

$$F(R)=f\sum_{j=1}^{N} d_j J_0(\pi d_j R), \tag{1}$$

where N is the number of walls and j denotes the jth shell. The equatorial line intensity was simulated by calculating $I(R)=|F(R)|^2$. Figure 2(a) shows the simulated equatorial layer line intensity which is sensitive to nanotube's inner diameter and the number of shells. We found that this carbon nanotube has five shells with chiral indices (i) (44, 18), (ii) (52, 20), (iii) (58, 22), (iv) (65, 25), and (v) (72, 28) as listed in Table I, where the metallicity (S: semiconductor; M: metal), diameter d, and helicity α are also given. It is interesting to note that all the shells have almost the same helicity and especially that the second shell (52,20) and the fourth shell (65,25) have the same helicity which caused the breakdown of the 2mm symmetry in the diffraction pattern.[25] In order to further confirm this, the first layer line intensity profile was also simulated. Although only two shells have the same v/u ratio, the positions of the first layer lines from all the shells are actually very close to each other. In our simulations, we used[25]

TABLE I. Chiral indices (u,v), metallicity, diameter d, and helicity α of each shell of the five-shell carbon nanotube shown in Fig. 1(a).

Shell No.	(u,v)	Metallicity	d (nm)	α (deg)
1	(44,18)	S	4.327	16.38
2	(52,20)	S	5.042	15.60
3	(58,22)	M	5.607	15.43
4	(65,25)	S	6.303	15.60
5	(72,28)	S	6.999	15.74

$$I(R,\Phi,l_1)=x_0^2f^2\sum_{j=1,3,5}|d_jJ_{v_i}(\pi d_jR)|^2+I_{2,4}(R,\Phi,l_1) \tag{2}$$

and

$$\begin{aligned}I_{2,4}(R,\Phi,l_1)=x_0^2f^2\{&|d_2J_{v_2}(\pi d_2R)|^2+|d_4J_{v_4}(\pi d_4R)|^2\\&+2d_2d_4J_{v_2}(\pi d_2R)J_{v_4}(\pi d_4R)\cos[(v_4-v_2)\\&\times(\Phi+\pi/2)+\Delta\varphi]\}\end{aligned} \tag{3}$$

to obtain the intensity profile of the first layer line [l_1, formed by the graphene (01) reflection] and the results are plotted in Figs. 2(b) and 2(c), respectively. It clearly shows that $I(R,\Phi+\pi,l_1)\neq I(R,\Phi,l_1)$, indicating a breakdown of the 2mm symmetry as observed experimentally.

Field emission measurements were carried out in a vacuum chamber operated at 3×10^{-8} torr. The fiber-carbon nanotube emitter was first positioned 400 μm away from the flat anode. A Cs metal dispenser (from SAES) was then carefully positioned so that the Cs beam was aimed at the nanotube. When the dispenser was heated up to 600 °C, the Cs atoms were released and deposited on the nanotube.

The field emission measurements were first obtained from the pristine nanotube at room temperature. The Fowler-Nordheim theory[26] describes the field emission process by giving the relationship between the current density J through a potential barrier, the applied voltage V, and the work function ϕ of the emitter surface,

$$J=1.5\times10^{-6}\frac{F^2}{\phi}\exp\left[\frac{10.4}{\phi^{1/2}}-\frac{6.44\times10^7\phi^{3/2}}{F}\right], \tag{4}$$

where

$$F=\beta V, \tag{5}$$

with F being the electric field and β the field enhancement factor. In the Fowler-Nordheim plot [$\ln(I/V^2)$ vs $1/V$)], the slope is $-6.44\times10^7\phi^{3/2}/\beta$. Since the field enhancement fac-

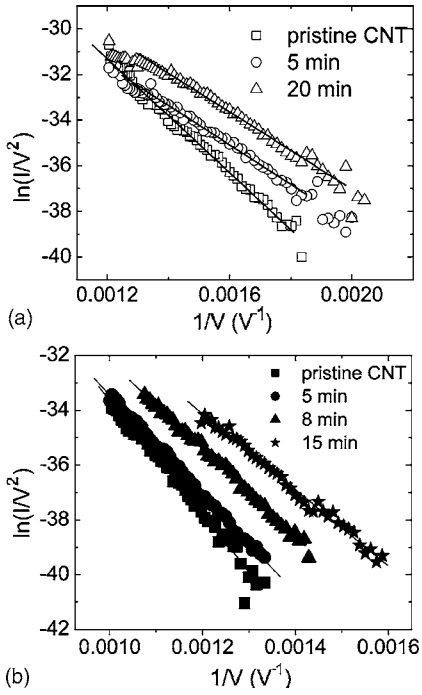

FIG. 3. (a) Fowler-Nordheim plot of the electron emission data from the single carbon nanotube [Fig. 1(a)] at different deposition times of Cs doping (square: pristine nanotube, circle: 5 min, and triangle: 20 min). (b) Fowler-Nordheim plot of the electron emission data from another single carbon nanotube with varying time of Cs doping (solid square: pristine nanotube, solid circle: 5 min, solid triangle: 8 min, and solid star: 15 min).

tor β is constant, the slope of the Fowler-Nordheim plot is only proportional to $\phi^{3/2}$. We deduced the work function of the Cs-doped carbon nanotube by comparing the slope of the Fowler-Nordheim plots for a pristine carbon nanotube with the slope for the same nanotube exposed to Cs. The field emission was measured three times to ensure that the Fowler-Nordheim plot was stable and reproducible. All three measurements agreed well and gave a field enhancement factor $\beta=3.4\times10^6$ m^{-1} with a work function of 4.8 eV for the pristine carbon nanotube as obtained from the generalized gradient approximation (GGA) calculations and measurements for both metallic and semiconducting nanotubes.[27,28]

Due to its extreme small dimensions, we were not able to measure precisely the concentration of Cs on the single carbon nanotube. Instead, we used the deposition time to label the concentration of Cs. Several sets of field emission data at different deposition times (5 min, 20 min) were collected and shown in the Fowler-Nordheim plot [$\ln(I/V^2)$ vs $1/V$] to allow comparisons with the pristine nanotube [Fig. 3(a)]. As the deposition time increased, the slopes of Fowler-Nordheim plots decreased significantly suggesting that the work function had been reduced. The ratio of the slope for the pristine nanotube and that for the nanotube exposed to Cs for 20 min is 1.43, which led to the reduction of the work function of the carbon nanotube from 4.8 to 3.8 eV. After 20 min of Cs exposure, the slope of the Fowler-Nordheim plot stopped decreasing, indicating that the concentration of Cs had reached saturation. We also measured the work function of another Cs-doped single carbon nanotube; the work function was reduced from 4.8 to 3.7 eV [Fig. 3(b)]. We noticed that this result is different from that reported by Suzuki *et al.*[14] where the Cs deposition decreased the work function of multiwalled carbon nanotubes by 2.2 eV. We attribute this difference to the lower concentration of Cs in the single carbon nanotube compared to nanotube bundles.[29] In our experiments, the field emission properties of the single Cs-doped carbon nanotube were measured multiple times over a period of more than 2 h and Cs desorption at high emission current was not observed in our experiments.

In the process of Cs doping, we believe that the Cs atoms were mostly deposited on the outermost shell and the tip of the carbon nanotube. As a result, the Fermi energy of the carbon nanotube is shifted toward the vacuum level to lower its work function.

In summary, the chiral indices of a five-shell carbon nanotube have been determined which has four semiconducting shells and one metallic shell in the middle (Table I). The work function for this nanotube has been measured as a function of Cs doping and we found that the work function of this nanotube was reduced from 4.8 to 3.8 eV due to the Cs doping.

The authors wish to thank financial support from Xintek/DOE SBIR and UNC Research Council. One of the authors (J.T.) is also partially supported by the JSPS Japan-US Collaborative Scientific Program.

[1] A. G. Rinzler, J. H. Hafner, P. Nikolaev, L. Lou, S. G. Kim, D. Tomanek, P. Nordlander, D. T. Colbert, and R. E. Smalley, Science **269**, 1550 (1995).
[2] W. A. de Heer, A. Chatelain, and D. Ugarte, Science **270**, 1179 (1995).
[3] J. M. Bonard, J. P. Salvetat, T. Stöckli, L. Forró, and A. Chatelain, Appl. Phys. A: Mater. Sci. Process. **69**, 245 (1999).
[4] W. B. Choi, D. S. Chung, J. H. Kang, H. Y. Kim, Y. W. Jin, I. T. Han, Y. H. Lee, J. E. Jung, N. S. Lee, G. S. Park, and J. M. Kim, Appl. Phys. Lett. **75**, 3129 (1999).
[5] N. de Jonge, Y. Lamy, K. Schoots, and T. H. Oosterkamp, Nature (London) **420**, 393 (2002).
[6] G. Z. Yue, Q. Qiu, B. Gao, Y. Cheng, J. Zhang, H. Shimoda, S. Chang, J. P. Lu, and O. Zhou, Appl. Phys. Lett. **81**, 355 (2002).
[7] M. J. Fransen, Th. L. Van Rooy, and P. Kruit, Appl. Surf. Sci. **146**, 312 (1999).
[8] N. de Jonge, J. Appl. Phys. **95**, 673 (2004).
[9] R. Gao, Z. Pan, and Z. L. Wang, Appl. Phys. Lett. **78**, 1757 (2001).
[10] N. de Jonge, M. Allioux, M. Doytcheva, M. Kaiser, K. B. K. Teo, R. G. Lacerda, and W. I. Milne, Appl. Phys. Lett. **85**, 1607 (2004).
[11] N. de Jonge, M. Allioux, J. T. Oostveen, K. B. K. Teo, and W. I. Milne, Phys. Rev. Lett. **94**, 186807 (2005).
[12] J. M. Macaulay, I. Brodie, C. A. Spindt, and C. E. Holland, Appl. Phys. Lett. **61**, 997 (1992).
[13] M. W. Geis, J. C. Twichell, J. Macaulay, and K. Okano, Appl. Phys. Lett. **67**, 1328 (1995).
[14] I. Brodie and P. R. Schwoebel, Proc. IEEE **82**, 1006 (1994).
[15] S. Suzuki, C. Bower, Y. Watanabe, and O. Zhou, Appl. Phys. Lett. **76**, 4007 (2000).
[16] A. Wadhawan, R. E. Stallcup, and J. M. Perez, Appl. Phys. Lett. **78**, 108 (2001).
[17] S. Suzuki, Y. Watanabe, T. Kiyokura, K. G. Nath, T. Ogino, S. Heun, W. Zhu, C. Bower, and O. Zhou, Surf. Rev. Lett. **9**, 431 (2002).
[18] L.-C. Qin and S. Iijima, Mater. Lett. **30**, 311 (1997).
[19] L.-C. Qin, J. Mater. Res. **9**, 2450 (1994).
[20] A. A. Lucas, V. Bruyninckx, and Ph. Lambin, Europhys. Lett. **35**, 355 (1996).
[21] M. Gao, J. M. Zuo, R. D. Twesten, I. Petrov, L. A. Nagahara, and R. Zhang, Appl. Phys. Lett. **82**, 2703 (2003).
[22] Z. Liu, Q. Zhang, and L.-C. Qin, Appl. Phys. Lett. **86**, 191903 (2005).
[23] L.-C. Qin, Rep. Prog. Phys. **69**, 2761 (2006).
[24] J. C. Meyer, M. Paillet, G. S. Duesberg, and S. Roth, Ultramicroscopy **106**, 176 (2006).
[25] Z. Liu and L.-C. Qin, Chem. Phys. Lett. **400**, 430 (2004).
[26] I. Brodie and C. A, Spindt, Adv. Electron. Electron Phys. **83**, 11 (1992).
[27] J. Zhao, J. Han, and J. P. Lu, Phys. Rev. B **65**, 193401 (2002).
[28] S. Suzuki, Y. Watanabe, Y. Homma, F. Fukuba, S. Heun, and A. Locatelli, Appl. Phys. Lett. **85**, 127 (2004).
[29] S. Suzuki and M. Tomita, J. Appl. Phys. **79**, 3739 (1996).